Talanta 97 (2012) 456–461

Contents lists available at SciVerse ScienceDirect

Talanta

journal homepage: www.elsevier.com/locate/talanta

Novel chitosan-based fluorescent materials for the selective detection and adsorption of Fe^{3+} in water and consequent bio-imaging applications

Qingtao Meng, Weiping Su, Cheng He, Chunying Duan*

State Key Laboratory of Fine Chemicals, Dalian University of Technology, 2 Linggong Road, Dalian High-Tech Industrial Zone, Dalian 116024, China

ARTICLE INFO

Article history:
Received 7 December 2011
Received in revised form
21 April 2012
Accepted 30 April 2012
Available online 1 June 2012

Keywords:
Chitosan
Fe^{3+}
Detection
Absorbent
Fluorescence imaging

ABSTRACT

A series of fluorescent materials were synthesized by modification of chitosan (CS) with 4-fluorescein-carboxaldehyde (Fluo) and N-methyl-carbazole-3-aldehyde (Cb). Both **L-CS-Fluo** and **L-CS-Cb** feature excellent water-solubility and exhibit highly selective fluorescence response to Fe^{3+} in environment and biological fields. The high-molecular weight chitosan-based materials: **H-CS-Fluo** and **H-CS-Cb** take on doubled absorptivity compared to free chitosan due to the introduction of fluorescence probes. These modified-probe chitosan materials could be regenerated by treating with EDTA. Meanwhile, monomer probes **AG-Fluo** and **AG-Cb** linked by D-glucosamine were also synthesized to explore the binding efficiency.

1. Introduction

Iron is the most abundant transition metal ion present in the earth's crust with average content of approximately 5% in soil, sediment and rocks [1]. It is also an essential trace element that plays significant roles in chemical and biological processes [2–5]. For example, Fe^{3+} provides the oxygen-carrying capacity of heme and acts as a cofactor in many enzymatic reactions involved in the mitochondrial respiratory chain, and both its deficiency and excess can induce a variety of diseases [6–8]. The drinking water standard for the maximum allowable level of Fe^{3+} in China is no more than 0.3 ppm [9]. Therefore, detection of Fe^{3+} in environmental and biological fields has aroused wide concern. Traditional detection methods, such as absorption spectrometry (AAS), inductively coupled plasma emission spectrometry (ICP-ES) and total reflection X-ray fluorimetry (TXRF) offer good limits of detection and wide linear ranges, but are very expensive and do not easily lend themselves to miniaturization [10]. Fluorescence probe is one of the best choices due to its high sensitivity and simplicity which translates molecular recognition information into tangible fluorescence signals [11]. Particularly, fluorescence probes are convenient to image intravital heavy transition metal (HTM) ions by *in situ* method. Currently, enormous efforts have been devoted to the development of Fe^{3+}-specific fluorescence probes [12,13]. However, most of them exhibited poor water solubility or biocompatibility restricting their applications. Moreover, their use in related analytical techniques in the homogeneous phase is not suitable for the separation, removal and enrichment of HTM ions in environmental field [14–15]. In recent years, we and other researchers have explored a novel way to design and prepare improved sensing materials by modification of mesoporous silica with fluorescence probes. These fluorescent materials were not only able to recognize HTM ions with high selectivity and sensitivity by fluorimetric or colorimetric method, but also can remove HTM ions from water sample [16–18]. At present, the selection of appropriate carriers has been a hotspot of study in this field.

Chitosan is one of the most abundant naturally occurring amino-polysaccharides and has attracted attention because of its unique physiochemical characteristics and biological activities [19–20]. First, chitosan is a carbohydrate biopolymer derived from deacetylation of chitin, the main component of crustacean exoskeletons. Chitin's abundance is second only to cellulose among polysaccharides found on Earth [21]. Second, the high contents of amino and hydroxyl functional groups of chitosan were beneficial to covalently graft organic functional molecules [22]. Lastly, the outstanding biodegradability and low toxicity of chitosan make it a desirable carrier to build biomaterials. Accordingly, chitosan-based materials have been widely used in environment [23–25], drug delivery [26–27], optical devices [28–31] and biomedical fields [32].

Herein, we reported a series of fluorescent materials by modification of chitosan with fluorescence dyes. We envisioned that these fluorescent materials could be used as fluorescence

* Corresponding author. Tel.: +86 411 84986261.
E-mail address: cyduan@dlut.edu.cn (C. Duan).

0039-9140/$ - see front matter © 2012 Elsevier B.V. All rights reserved.
http://dx.doi.org/10.1016/j.talanta.2012.04.062

probes and adsorbent in environmental field and fluorescence imaging agent in biological field. Furthermore, related detection and adsorption processes could be monitored by fluorimetric or colorimetric response methods. Meanwhile, monomer probes **AG-Fluo** and **AG-Cb** linked by D-glucosamine were also synthesized to explore the bonding mechanism.

2. Experimental

2.1. Reagents and instruments

All reagents and solvents were of AR grade and used without further purification unless otherwise noted. D-Glucosamine hydrochloride, Chitosan and fluorescein were purchased from Sinopharm Chemical Reagent Co., Ltd. (China). Stock solution (2×10^{-2} M) of the aqueous nitrate salts of Fe^{3+}, Hg^{2+}, Cu^{2+}, Cd^{2+}, Pb^{2+}, Zn^{2+}, Ni^{2+}, Co^{2+}, Mn^{2+}, Cr^{3+}, Ag^{+}, Ca^{2+}, Mg^{2+}, Ba^{2+}, Li^{+}, K^{+}, Na^{+} were prepared for further experiments.

^{1}H-NMR and ^{13}C-NMR spectra were recorded with a Varian Inova-400 spectrometer with chemical shifts reported as ppm (in CD_3Cl, TMS as internal standard). Mass spectral determinations were made on an ESI-Q-TOF mass spectrometry (Micromass, UK). High resolution mass spectra measurements were performed on a GC-TOF mass spectrometry (Micromass, UK). FT-IR spectra were recorded on a Nicolet Magna-IR 750 spectrometer equipped with a Nic-Plan Microscope. UV–*vis* diffuse reflectance spectra were taken on a Shimadzu UV-2401PC spectrophotometer using $BaSO_4$ as the reference. Elemental analyses (C, H and N) were performed on an Elementary Vario EL analyzer. Fluorescence spectra were determined with FS920 luminescence spectrometer (Edinburgh Instruments). Absorption spectra were measured with Lambda 35 UV–vis spectrophotometer. All pH measurements were made with a Model PHS-3C meter. The adsorption ability of **H-CS-Fluo** and **H-CS-Cb** for Fe^{3+} in water was measured by Inductively Coupled Plasma Spectrometer (Perkin Elmer). Cells were imaged by Nikon eclipase TE2000-5 inverted fluorescence microscopy.

2.2. General procedures of spectra registration/spectrophotometric detection

Stock solutions of **AG-Fluo**, **AG-Cb**, **L-CS-Fluo** and **L-CS-Cb** were prepared in Tris-HCl buffer (0.02 M pH=7.2). The cationic solutions were all in water with a concentration of 2.0×10^{-2} M for spectrometric analysis. Excitation wavelength for **AG-Fluo** and **L-CS-Fluo** was 470 nm. Excitation wavelength for **AG-Cb** and **L-CS-Cb** was 350 nm for the fluorescence titration of Fe^{3+}. Before spectroscopic measurements, the solution was freshly prepared by diluting the high concentration stock solution to corresponding solution. Each time a 2 mL solution of probe was filled in a quartz cell of 3 cm optical path length, and different stock solutions of cations were added into the quartz cell gradually by using a micro-syringe. The volume of cationic stock solution added was less than 100 μL with the purpose of keeping the total volume of testing solution without obvious change.

2.3. Synthesis and characterization the fluorescent materials

2.3.1. Synthesis of 4-fluoresceincarboxaldehyde and N-methyl-carbazole-3-aldehyde

4-fluoresceincarboxaldehyde and N-methyl-carbazole-3-aldehyde were prepared according to reported procedures [33–34].

2.3.2. Synthesis of ***AG-Fluo***

30 mL methanol solution of 4-fluoresceincarboxaldehyde (0.99 g, 2 mmol) was added to the solution D-glucosamine·HCl (0.43 g, 2 mmol) and triethylamine (0.3 mL). The mixture was refluxed for 4 h under N_2. After cooling to room temperature, the solvent was removed under reduced pressure. The crude product was then purified by chromatography on a silica gel column (CH_2Cl_2:CH_3OH, 1:15, V/V) to give **AG-FLuo** as a yellow solid in 45% yield. Elemental analysis: calcd (%) for $C_{27}H_{23}NO_{10}$: C 62.19, H 4.45, N 2.69%. Found (%): C 62.21H 4.461N 2.716%. ESI-MS negative peak at m/z=522.0 indicated [**AG-Fluo**+H]$^{+}$. ^{1}H-NMR (400 MHz, DMSO-d_6) δ (ppm):10.30 (s, 1H), 9.08 (s, 1H), 8.07 (s, 1H), 7.86 (d, 1H), 7.79 (d, 1H), 7.34 (d, 1H), 7.04 (m, 1H), 6.88 (d, 1H), 6.72 (d, 1H), 6.61 (d, 1H), 6.38 (d, 1H), 5.47 (m, 1H), 5.42 (m, 1H), 5.33 (d, 1H), 5.18 (d, 1H), 4.86 (d, 1H), 4.63 (t, 1H), 3.84 (t, 1H), 3.73 (m, 1H), 3.65 (m, 2H), 3.55 (m, 1H), 3.33 (m, 1H), 3.25 (t, 1H). ^{13}C-NMR (100 MHz, DMSO-d_6): δ (ppm) 61.48, 67.74, 70.78, 71.61, 72.96, 74.83, 77.37, 91.22, 95.35, 102.89, 104.28, 110.16, 113.78, 115.78, 119.42, 124.52, 125.14, 129.49, 130.53, 133.05, 134.03, 136.10, 151.61, 160.82, 161.75, 169.22. IR (KBr): 3422 cm^{-1}, 2936 cm^{-1}, 1730 cm^{-1}, 1649 cm^{-1}, 1585 cm^{-1}, 1527 cm^{-1}, 1471 cm^{-1}, 1373 cm^{-1}, 1293 cm^{-1}, 1171 cm^{-1}, 1099 cm^{-1}, 1042 cm^{-1} and 581 cm^{-1}.

2.3.3. Synthesis of ***L-CS-Fluo***

4-fluoresceincarboxaldehyde (0.99 g, 2 mmol) was dissolved in 50 mL methanol. Then water-soluble low-molecular weight chitosan (L-CS) (2.0 g) was added. The mixture was refluxed for 8 h under N_2. After cooling to room temperature, the solvent was removed under reduced pressure. The resulting powder was dissolved in 20 mL methanol and washed with CH_2Cl_2/CH_3OH (1:15, V/V) on a silica gel chromatography to wash off the nonbounded 4-fluorescein-carboxaldehyde. Methanol was then added constantly until the yellow production drain away. The collected solution was evaporated in vacuum to afford yellow solid **L-CS-Fluo** in 48% yield. Elemental analysis: found (%): C 34.10, H 5.506, N 3.996. IR (KBr): 3442 cm^{-1}, 3006 cm^{-1}, 2920 cm^{-1}, 2744 cm^{-1}, 1629 cm^{-1}, 1520 cm^{-1}, 1383 cm^{-1}, 1290 cm^{-1}, 1245 cm^{-1}, 1206 cm^{-1}, 1140 cm^{-1}, 1080 cm^{-1}, 1022 cm^{-1}, 924 cm^{-1}, 812 cm^{-1}, 741 cm^{-1}, 573 cm^{-1} and 453 cm^{-1}.

2.3.4. Synthesis of ***H-CS-Fluo***

4-fluoresceincarboxaldehyde (0.99 g, 2 mmol) was dissolved in 50 mL methanol. Then high-molecular weight chitosan (H-CS) (2.0 g) was added. The mixture was refluxed for 8 h under N_2. After cooling to the room temperature and evaporated the solvent in vacuum. The resulting powder was then put into a Sechelt's extractor and extracted with methanol for at least 12 h to ensure that there was noncovalently bounded 4-fluoresceincarboxaldehyde in chitosan. After drying under reduced pressure, the reaction afforded **H-CS-Fluo** as yellow solid. Elemental analysis: found (%):C 43.45, H 6.661, N 7.085. IR (KBr): 3440 cm^{-1}, 2990 cm^{-1}, 2883 cm^{-1}, 1755 cm^{-1}, 1600 cm^{-1}, 1469 cm^{-1}, 1280 cm^{-1}, 1051 cm^{-1} and 463 cm^{-1}.

2.3.5. Synthesis of ***AG-Cb***

4-fluoresceincarboxaldehyde (0.99 g, 2 mmol), D-glucosamine·HCl (0.43 g, 2 mmol) and triethylamine (0.3 mL) were mixed in 30 mL methanol. After the solution was refluxed for 3 h with stirring, pale precipitates obtained were filtered, washed with cold methanol (3×5 mL) and dried under vacuum with 85% yield. Elemental analysis: calcd (%) for $C_{20}H_{22}N_2O_5$: C 64.85, H 5.99, N 7.56%. Found (%): C 64.24, H 5.95 and N 7.15%. ESI-MS positive peak at m/z 371.0 indicated [**AG-Cb**+H]$^{+}$. ^{1}H NMR (400 MHz, DMSO-d_6) δ (ppm): 8.51 (s, 1H), 8.34(s, 1H), 8.23 (s, 1H), 7.90 (d, 1H), 7.63 (d, 1H), 7.50 (t, 1H), 7.25 (t, 1H), 6.55 (d, 1H), 4.92 (d, 1H), 4.83 (d, 1H), 4.76 (t, 1H), 4.55 (t, 1H), 3.91 (s, 3H), 3.76 (m,

1H), 3.51 (m, 2H), 3.29 (m, 1H), 3.19 (m, 1H), 2.88 (t, 1 H), ^{13}C NMR (100 MHz, DMSO-d_6): δ (ppm) 40.12, 61.35, 70.47, 74.77, 76.90, 78.37, 95.78, 109.08, 109.48, 119.37, 120.45, 120.71, 121.96, 122.14, 125.93, 126.13, 127.60, 141.15, 141.97 and 162.53.

2.3.6. Synthesis of **L-CS-Cb** and **H-CS-Cb**

The synthesis methods of **L-CS-Cb** and **H-CS-Cb** were referred to **L-CS-Fluo** and **H-CS-Fluo**.

2.4. Adsorption ability of **H-CS-Fluo** and **H-CS-Cb** for Fe^{3+} in different water samples: laboratory pure water (LW), drinking water (DW) and seawater (SW)

H-CS-Fluo or **H-CS-Cb** (50 mg) and chitosan (50 mg) were added to the about 1 ppm Fe^{3+} solution (50 mL) prepared with above water samples, respectively. The mixture was stirred for 4 h. After filtration, the concentration of residual Fe^{3+} in the filtrate was analyzed by inductively coupled plasma source mass spectrometer (ICP).

2.5. Fluorescence imaging of MCF-7 cells with **AG-Fluo** and **L-CS-Fluo**

MCF-7 (Human Breast Cancer) cells were supplied by Institute of Environmental Systems Biology, Dalian Maritime University.

MCF-7 cells were incubated with **AG-Fluo** (10 μM, in PBS medium) and **L-CS-Fluo** (1 ppm, in PBS medium) for 15 min at 28 °C, respectively. After washing with PBS three times, MCF-7 cells were supplemented with Fe^{3+} (0.2 mM) for another 15 min, and were imaged by fluorescence microscopy, excited with green light.

2.6. Fluorescence imaging of MCF-7 cells with **AG-Cb** and **L-Cs-Cb**

MCF-7 cells incubated with **AG-Cb** (10 μM, in PBS medium) or **L-CS-Cb** (1 ppm, in PBS medium) for 15 minutes at 28 °C. After washing with PBS three times, MCF-7 cells were supplemented with Fe^{3+} (0.3 mM) for 15 min, and were imaged by fluorescence microscopy, excited with blue light.

2.7. The application of **L-CS-Fluo** for the detection of Fe^{3+} in spinach juice

For fluorescence measurements, a solution containing 2×10^{-2} M of Fe^{3+} (estimated by ICP) was first prepared by addition of $Fe(NO_3)_3$ to fresh spinach juice. Then, various amount of above Fe^{3+} were further added into the stock solution of **L-CS-Fluo**. Excitation was performed at 470 nm.

3. Results and discussion

3.1. Synthesis and characterization of the dye-modified chitosan materials

In this paper, we chose two types of chitosan materials: water-soluble (L-CS) and high-molecular weight (H-CS). Functional fluorescent materials **CS-Fluo** and **CS-Cb** were prepared by modification of chitosan with 4-fluoresceincarboxaldehyde and N-methylcarbazole-3-aldehyde, respectively. These materials were well characterized by UV–vis diffuse reflectance spectra, FT-IR spectra, Elemental Analysis (EA) and several fluorescence spectra. Corresponding monomolecular fluorescence probes **AG-Fluo** and **AG-Cb** (Scheme 1) were also synthesized by Schiff base-condensation reaction.

In order to make sure the fluorophores were successfully modified onto chitosan material, UV–vis diffuse reflectance spectra of L/H-CS, **L/H-CS-Fluo** and **L/H-CS-Cb** were compared. As shown in Fig. 1, a broad new band centered at 480 nm for both **L-CS-Fluo** and **H-CS-Fluo** were emerged (Fig. S1). This band was characteristic of fluorescein dye originating from the typical electronic transition of an aromatic ring and C=N conjugate system in a molecule of **CS-Fluo** [35–38]. Analogously, the new band centered at 360 nm for **L-CS-Cb** and **H-CS-Cb** could be attributed to the modified carbazole dye. For further proofs, FT-IR spectroscopy of chitosan and its derivatives were compared. As shown in Figs. S2 and S3, a series of new characteristic bands mainly centered at 1745 cm^{-1}, 1606 cm^{-1}, 1470 cm^{-1} and 1330 cm^{-1} emerged for **L-CS-Fluo** and **H-CS-Fluo**, indicating that fluorescein dyes were successfully linked to chitosan material. Similarly, several new absorption peaks appeared for **L-CS-Cb** and **H-CS-Cb** at 3030 cm^{-1}, 2900 cm^{-1}, 1680 cm^{-1}, 1600 cm^{-1},

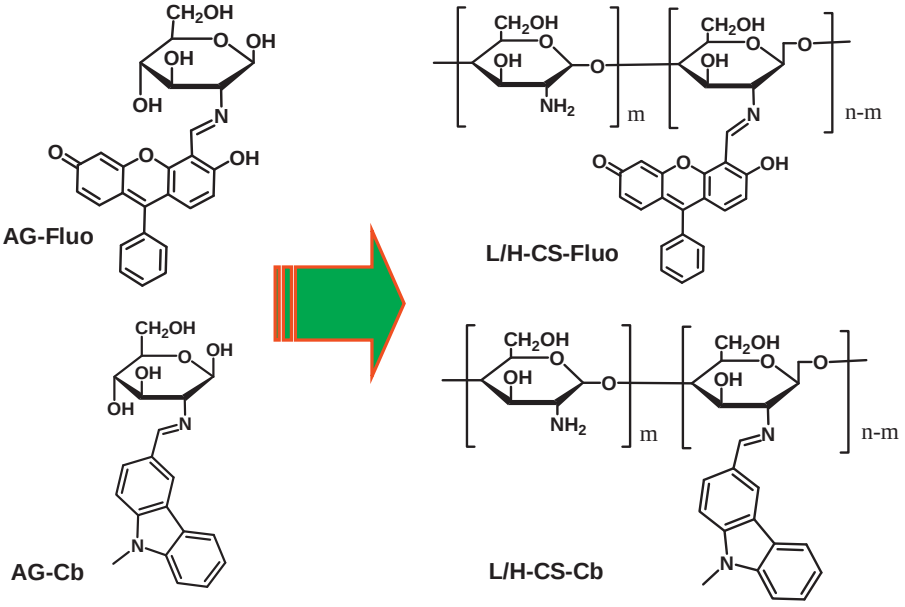

Scheme 1. Schematic diagram of chitosan-based fluorescent materials: "Molecule" to "Material".

1470 cm^{-1}, 1320 cm^{-1}, 1240 cm^{-1}, 1140 cm^{-1}, 810 cm^{-1} and 750 cm^{-1} also providing rich evidences for the successful connection of carbazole dye with chitosan (Figs. S4 and S5) [39–40].

3.2. The application of probe-modified chitosan fluorescent materials for the detection and adsorption of Fe^{3+} in water

Fluorescent material **L-CS-Fluo** features excellent water-solubility and displayed strong green fluorescence at 516 nm in Tris-HCl buffered 100% water solution at pH 7.2 (Fig. 2). With 0.3 mM of Fe^{3+}, fluorescence intensity of **L-CS-Fluo** (5 ppm) was almost completely quenched (quenching efficiency at 516 nm was 94%), which could be ascribed to a PET (photo-induced energy transfer) mechanism and/or a paramagnetic quenching effect of Fe^{3+} [41–44]. Moreover, no significant spectral changes of **L-CS-Fluo** occurred in the presence of alkali or alkaline, earth metals and the first-row transition metals, such as Li^+, K^+, Na^+, Ca^{2+}, Mg^{2+}, Ba^{2+}, Cd^{2+}, Pb^{2+}, Zn^{2+}, Ni^{2+}, Co^{2+}, Mn^{2+}, Ag^+. Although the fluorescence responses of **L-CS-Fluo** were mildly disturbed by Cu^{2+} and Hg^{2+}, upon addition of 1 equiv. of Fe^{3+} to the above solution giving rise to drastic quenching in accordance with the addition of 1 equiv. of Fe^{3+} alone, indicating that Fe^{3+}-specfic responses were not disturbed by competitive ions (Fig. 3). The detection limit of **L-CS-Fluo** for Fe^{3+} in water was established at 0.2 ppm under current experimental conditions (Fig. S6). We also investigated the application of **L-CS-Fluo** in the analysis of Fe^{3+} in real biological samples. As shown in Fig. S7, the fluorescence quenching degree is still linear to the concentration of Fe^{3+} in the range of 0–0.6 ppm with a detection limit of 0.4 ppm in spinach juice. Therefore, we believed that **L-CS-Fluo** could be potentially used to monitor excess Fe^{3+} in water and biological samples.

Similarly, fluorescent material **L-CS-Cb** was also able to selectively detect Fe^{3+} by fluorescent quenching method in Tris-HCl buffer. Upon addition 0.5 mM of Fe^{3+} to the solution of **L-CS-Cb** (0.2 g/L), the green fluorescence emission at 508 nm was quenched by 60% (Fig. 4), and Fe^{3+}-specfic fluorescence responses were not disturbed by competitive ions (Fig. S8). The detection limit of **L-CS-Cb** for Fe^{3+} was established at 0.6 ppm under current experimental conditions.

To further realize the practical environmental application as absorbent for Fe^{3+} in water, we then designed and synthesized high-molecular weight chitosan-based functional material: **H-CS-Fluo** and **H-CS-Cb**. These functional materials were used in a heterogeneous phase which was convenient for removing toxic metal ions from pollutant solution. In addition, the bonding ability of **H-CS-Fluo** and **H-CS-Cb** to Fe^{3+} could be enhanced in comparison with free chitosan due to the combination of Fe^{3+}-specific fluorescence probes.

1 *ppm* Fe^{3+} in 50 mL pure water was treated with 50 mg **H-CS-Fluo** for 4 h. After filtration, the concentration of Fe^{3+} solution before and after treating with **H-CS-Fluo** was estimated by inductively coupled plasma source mass spectrometer (ICP). As shown in Fig. 5, **H-CS-Fluo** adsorbed about 96% of Fe^{3+}, only 47% of Fe^{3+} was adsorbed by free chitosan (H-CS) under the same condition. Moreover, **H-CS-Fluo** showed a stable absorptivity in

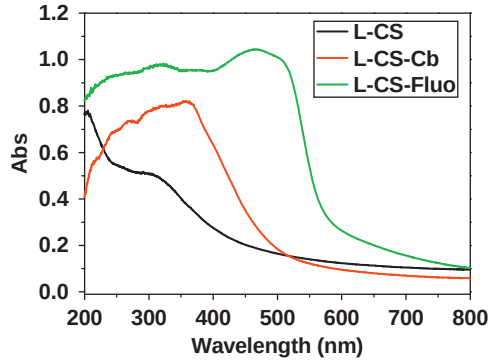

Fig. 1. UV–vis diffuses reflectance spectra of **L-CS-Fluo** and **L-CS-Cb**.

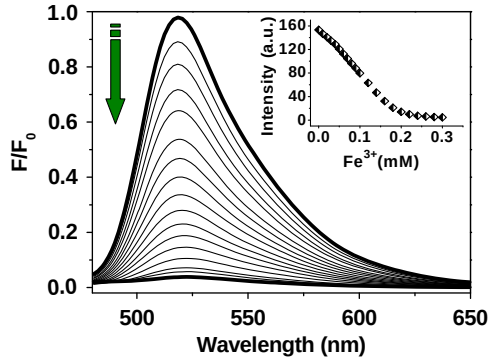

Fig. 2. Fluorescence spectra of **L-CS-Fluo** (5 ppm) in Tris-HCl buffer (0.02 M, pH=7.2) in the presence of different amounts of Fe^{3+} (0–0.3 mM). Excitation was performed at 470 nm.

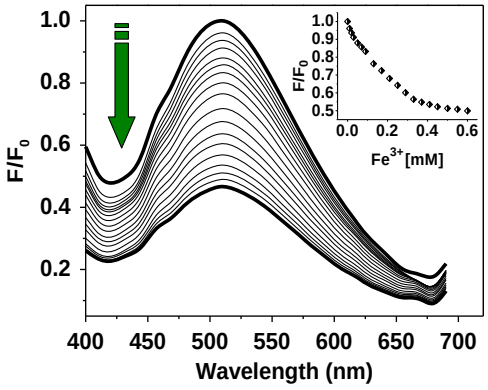

Fig. 4. Fluorescence spectra of **L-CS-Cb** (0.2 g/L) in Tris–HCl buffer (0.02 M, pH=7.2) in the presence of different amounts of Fe^{3+} (0–0.6 mM). Excitation was performed at 350 nm.

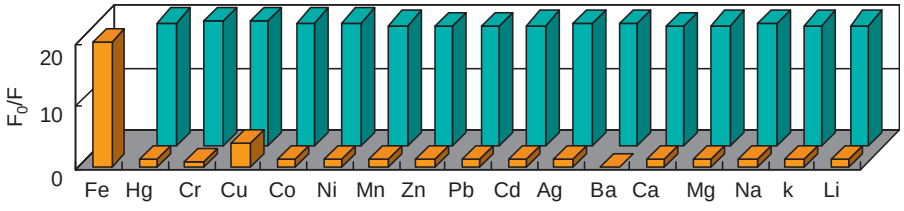

Fig. 3. Normalized fluorescence quenching degree of **L-CS-Fluo** (5 ppm) to various cations in Tris-HCl buffer (20 mM, pH=7.2). The front bars represent the fluorescence quenching degree of **L-CS-Fluo** in the presence of cations of interest (all are 0.3 mM). The back bars represent the quenching degree of the emission that occurs upon the subsequent addition of 0.3 mM of Fe^{3+} to the above solution. The intensities were recorded at 516 nm (F_0/F), excitation at 470 nm.

different water source samples indicating its favorable practical ability. Functional material **H-CS-Cb** is also an efficient adsorbent for Fe^{3+} in different water samples (Fig. S9). Both **H-CS-Fluo** and **H-CS-Cb** could be regenerated by treating with EDTA (Figs. S10 and S11). Therefore, we believe that **H-CS-Fluo** and **H-CS-Cb** are excellent absorbents for the excess Fe^{3+} in industrial wastewater.

In order to explore the binding mode, we then study the detection ability of **AG-Fluo** for Fe^{3+} in water. As shown in Fig. 6, the solution of **AG-Fluo** (10 μM) also showed strong green fluorescence emission at 516 nm in accord with **L-CS-Fluo**. Upon addition of Fe^{3+} (0.2 mM), the fluorescence intensity reached its equilibrium and 97% of the fluorescence was quenched (Fig. 6, insert). According to reported works, we concluded that **AG-Fluo** forms a 1:1 complex with Fe^{3+} and the association constant (Ka) being calculated as $2.20\times10^{6}\ M^{-1}$ [45]. Furthermore, the detection limit of **AG-Fluo** for Fe^{3+} was also established at 0.2 ppm under current experimental conditions.

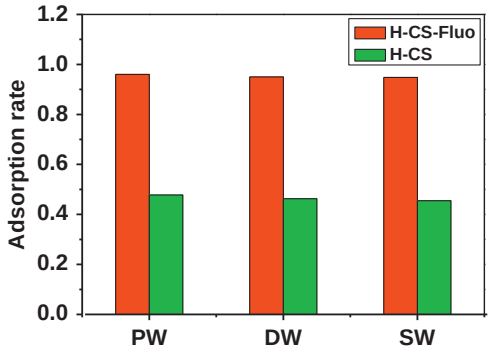

Fig. 5. The adsorption ability of H-CS (100 mg) and **H-CS-Fluo** (100 mg) for Fe^{3+} (1 ppm) in different water samples: laboratory pure water (LW), drinkingwater (DW) and seawater (SW).

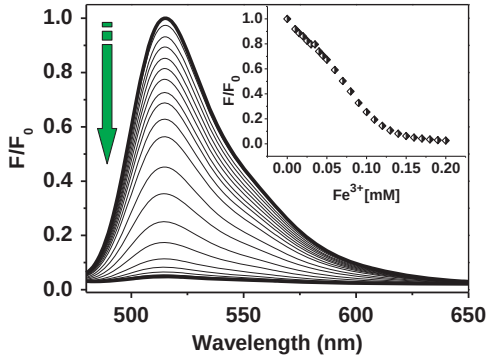

Fig. 6. Normalized fluorescence spectra of **AG-Fluo** (10 μM) in Tris-HCl buffer (0.02 M pH=7.2) in the presence of different amounts of Fe^{3+} (0.2 mM). Excitation was performed at 470 nm.

AG-Fluo also features excellent selectivity towards Fe^{3+} over other competitive cations species in Tris–HCl buffer. Upon addition of competitive cations (0.2 mM) to the solution of **AG-Fluo** (10 μM), the quenching rate of the emission intensities recorded at 516 nm (F_0/F) were shown in Fig. 7. No significant changes of the fluorescence intensities occurred in the presence of Li^+, K^+, Na^+, Ca^{2+}, Mg^{2+}, Ba^{2+}, Cd^{2+}, Pb^{2+}, Zn^{2+}, Ni^{2+}, Co^{2+}, Mn^{2+} and Ag^+. Although a mild fluorescence quenching was also detected after addition of Cu^{2+} and Hg^{2+}, the addition of Fe^{3+} ions to the above suspensions gave rise to drastic quenching of their fluorescence intensities, revealing that Fe^{3+} has the strongest binding affinity to **AG-Fluo** and the Fe^{3+}-specific response was not disturbed by the competitive ions.

The detection ability of **AG-Cb** was also consistent with **L-CS-Cb**. As shown in Fig. 8, about 80% of the fluorescence intensity of **AG-Cb** was quenched upon addition of 0.6 mM Fe^{3+} with an association constant (Ka) being calculated as $1.30\times10^{4}\ M^{-1}$ and the fluorescence response was not disturbed by competitive ions, revealing that **AG-Cb** features high affinity to Fe^{3+} over other metal ions (Fig. S12). The detection limit of **AG-Cb** for Fe^{3+} was established at only 0.6 ppm under current experimental conditions owing to less coordination sites compared with the case of **AG-Fluo**.

The states of Fe^{3+} ion were sensitive to the pH [46–48], and fluorescence dyes were usually disturbed by the proton in the detection of metal ions in water. Accordingly, pH titration was measured. As shown in Figs. S13 and S14, both **L-CS-Fluo** and **L-CS-Fluo** had stable fluorescence properties over a wide pH span of 5.0–9.0, revealing that they are suitable for application under physiological conditions.

We believe that the introduction of water-soluble chitosan to the fluorescence probe will facilitate its membrane penetration and biocompatibility. MCF-7 cells were firstly incubated with 1 *ppm* **L-CS-Fluo** for 30 min at 37 °C, then washed with PBS three times and mounted on a microscope stage. As shown in Fig. 9(a), the cells displayed strong green fluorescence, suggesting that

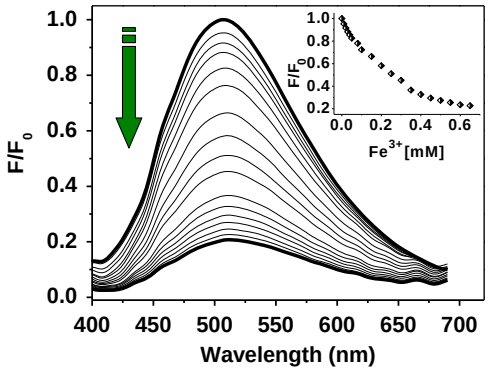

Fig. 8. Fluorescence spectra of **AG-Cb** (10 μM) in Tris-HCl (0.02 M, pH=7.2) buffer upon addition of different amounts of Fe^{3+} (0–0.6 mM), excitation at 350 nm.

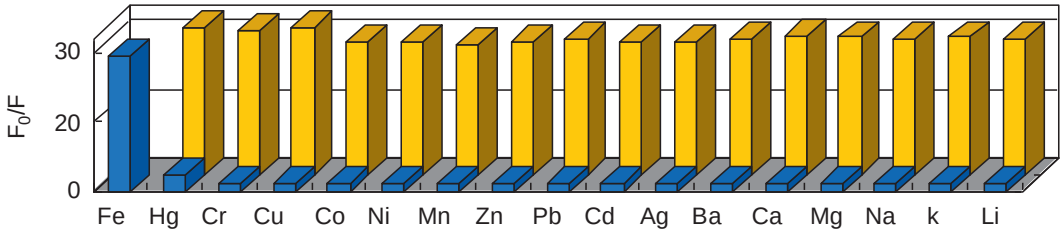

Fig. 7. Normalized fluorescence quenching degree of **AG-Fluo** (10 μM) to various cations in Tris-HCl buffer (0.02 M, pH=7.2). The front bars represent the quenching degree of **AG-Fluo** in the presence of cations of interest (all are 0.2 mM). The back bars represent the quenching degree of the emission that occurs subsequent upon the addition of 0.2 mM of Fe^{3+} to the above solution. The intensities were recorded at 516 nm (F_0/F), excitation at 470 nm.

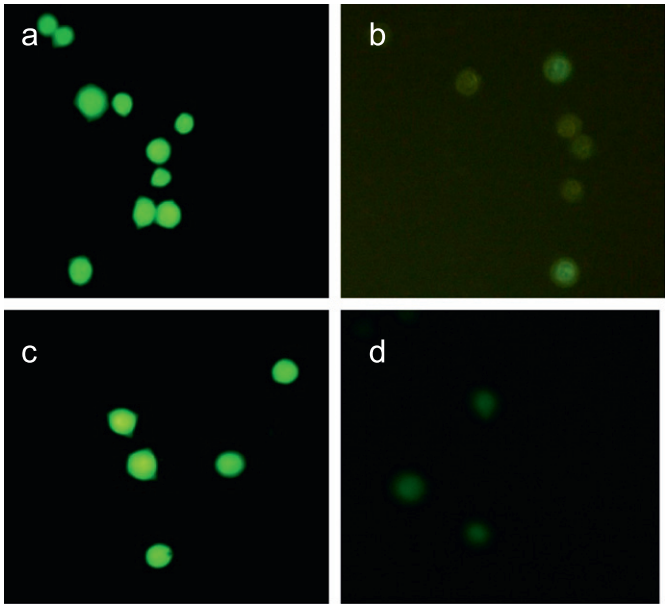

Fig. 9. Fluorescence images of Fe^{3+} in living MCF-7 cells. (a) Fluorescence image of MCF-7 cells incubated with **L-CS-Fluo** (1 ppm); (b) fluorescence image of MCF-7 cells incubated with **L-CS-Fluo**, and further incubated with Fe^{3+} (0.1 mM), excited with green light. (c) Fluorescence image of MCF-7 cells incubated with **L-CS-Cb** (1 ppm); (d) fluorescence image of MCF-7 cells incubated with **L-CS-Cb**, and further incubated with Fe^{3+} (0.3 mM), excited with blue light.

L-CS-Fluo was efficiently taken up into cells [49]. In contrast, a quenching fluorescence in the cells was observed by further addition of Fe^{3+} (0.1 mM) indicating that the intracellular Fe^{3+} ions were detected by **L-CS-Fluo** (Fig. 9b). MCF-7 cells incubated with 1 ppm **L-CS-Cb** also showed a clear green intracellular fluorescence (Fig. 9c). When MCF-7 cells were further incubated with 0.3 mM Fe^{3+} for 30 min, a remarkable quenching of the fluorescence intensity was also observed (Fig. 9d). According to above results, we concluded that probe-modified chitosan materials could be used as fluorescence imaging agent in biological and biomedicine fields. Analogously, their monomers, **AG-Fluo** and **AG-Cb** could be also used to monitor intracellular Fe^{3+} by fluorescence imaging method (Figs. S15 and S16).

4. Conclusions

In conclusion, we have reported two biocompatibility fluorescent materials (**L-CS-Fluo** and **L-CS-Cb**) based on water-soluble chitosan which can selectively and sensitively detect of Fe^{3+} in water and living cells. The insoluble material **H-CS-Fluo** and **H-CS-Cb** can be used as a high-efficiency absorbent to remove excess Fe^{3+} ions from water. We believe that chitosan-based fluorescent materials should have wide uses in environmental and biological field.

Appendix A. Supplementary information

Supplementary data associated with this article can be found in the online version at http://dx.doi.org.10.1016/j.talanta.2012.04.062

References

[1] H.J. Hapke, in: E. Merian (Ed.), Ed.,VCH Weinheim, New York, 1991 469–479.
[2] B.J. Halliwell, Neurochem 59 (1992) 1609–1623.
[3] E.D. Weinberg, Eur. J. Cancer Prev. 5 (1996) 19–22.
[4] D. Galaris, V. Skiada, A. Barbouti, Cancer Lett. 266 (2008) 21–29.
[5] S. Waminathan, A.V. Fonseca, G.M. Alam, V.S. Shah, Diabetes Care 30 (2007) 1926–1929.
[6] R.M. Berne, M.N. Levy, Physiology, 3rd ed., St. Louis, Mosby, 1988.
[7] J.T. Rogers, A.I. Bush, H.H. Cho, D.H. Smith, A.M. Thomson, A.L. Friedlich, D.K. Lahiri, P.J. Leedman, X. Huang, C.M. Cahill, Biochem. Soc. Trans. 36 (2008) 1282.
[8] L. Silvestri, C.J. Camaschella, Cell Mol. Med. 12 (2008) 1548–1550.
[9] M. E. P. of, P R China, National Standards for the Daily Drinking Water Quality 2007.
[10] G. Ozturk, S. Alp, K. Ertekin, Dyes and Pigm. 72 (2007) 150–156.
[11] M. Kumar, R. Kumar, V. Bhalla, Org. Lett. 13 (2011) 366–369.
[12] C.R. Lohani, J. Kim, K. Lee, Bioorg. Med. Chem. Lett. 19 (2009) 6069–6073.
[13] W. Lin, L. Yuan, J. Feng, X. Cao, Eur. J. Org. Chem. 16 (2008) 2689–2692.
[14] H.Y. Lee, D.R. Bae, J.C. Park, H. Song, W.S. Han, J.H. Jung, Angew. Chem. Int. Ed. 48 (2009) 1239–1243.
[15] S.J. Lee, S.S. Lee, M.S. Lah, J. Hong, J.H. Jung, Chem. Commun. 43 (2006) 4539–4541.
[16] Q.T. Meng, X.L. Zhang, C. He, G.J. He, P. Zhou, C.Y. Duan, Adv. Funct. Mater. 20 (2010) 1903–1909.
[17] H.J. Kim, S.J. Lee, S.Y. Park, J.H. Jung, J.S. Kim, Adv. Mater. 20 (2008) 3229–3234.
[18] Q.T. Meng, W.P. Su, X.M. Hang, X.Z. Li, C. He, C.Y. Duan, Talanta 86 (2011) 408–414.
[19] R.A.A. Muzzarelli, Carbohydr. Polym. 3 (1983) 53–75.
[20] K. Kurita, Prog. Polym. Sci. 26 (2001) 1921–1971.
[21] H. Tang, P. Zhang, T.L. Kiefta, S.J. Ryan, S.M. Baker, W.P. Wiesmann, S. Rogelj, Acta Biomater. 6 (2010) 2562–2571.
[22] G.L. Martin, J.A. Ross, S.D. Minteer, D.M. Jameson., M.J. Cooney, Carbohydr. Polym. 77 (2009) 695–702.
[23] S. Lai, X. Chang, C. Fu, Microchim. Acta 165 (2009) 39–44.
[24] E. Renbutsu, S. Okabe, Y. Omura, F. Nakatsubo, S. Minami, H. Saimoto, Y. Shigemasa, Carbohydr. Polym. 69 (2007) 697–706.
[25] W.S. Wan Ngah, C.S. Endud, R. Mayanar, React. Funct. Polym. 50 (2002) 181–190.
[26] B. Wilson, M.K. Samanta, K. Santhi, K.P.S. Kumar, M. Ramasamy, M. Pharmc, B. Suresh, Nanomed.: Nanotechnol., Biol. Med. 6 (2010) 144–152.
[27] R. Guo, L. Zhang, H. Qian, R. Li, X. Jiang, B. Liu, Langmuir 26 (2010) 5428–5434.
[28] M. Nowakowska, Ł. Moczek, K. Szczubiałka, Biomacromolecules 9 (2008) 1631–1636.
[29] Q. Yang, L. Shuai, X. Pan, Biomacromolecules 9 (2008) 3422–3426.
[30] W. Guo, Z. Ye, G. Wang, X. Zhao, J. Yuan, Y. Du, Talanta 78 (2009) 977–982.
[31] C. Lim, S. Kim, I.C. Kwon, Ahn, C.S.Y. Park, Chem. Mater. 21 (2009) 5819–5825.
[32] F. Manakker, T. Vermonden, C.F. Nostrum, W.E. Hennink, Biomacromolecules 10 (2009) 3157–3175.
[33] W. Liu, L. Xu, R. Sheng, P. Wang, H. Li, S. Wu, Org. Lett. 9 (2007) 2832–3829.
[34] Y. Gao, J. Wu, M. Li, P. Sun, H. Zhou, J. Yang, S. Zhang, B. Jin, Y. Tian, J. Am. Chem. Soc. 131 (2009) 5208–5213.
[35] X. Chen, H. Ma, Anal. Chim. Acta 575 (2006) 217–222.
[36] R.M. Kierat, R. Krämer, Bioorg. Med. Chem. Lett. 15 (2005) 4824–4827.
[37] M.G. Choi, S. Cha, H. Lee, H.L. Jeon, S. Chang, Chem. Commun. (2009) 7390–7392.
[38] C. Lim, S. Kim, I.C. Kwon, C. Ahn, S.Y. Park, Chem. Mater. 21 (2009) 5819–5825.
[39] M.G. Sandros, M. Behrendt, D. Maysinger, M. Tabrizian, Adv. Funct. Mater. 17 (2007) 3724–3730.
[40] C. Zhang, Q. Ping, H. Zhang, J. Shen, Eur. Polym. J. 39 (2003) 1629–1634.
[41] M. Kumar, R. Kumar, V. Bhalla, Org. Lett. 12 (2010) 366–369.
[42] J.P. Sumner, R. Kopelman, Analyst 130 (2005) 528–533.
[43] Y. Ma, W. Luo, P.J. Quinn, Z. Liu, R.C.J. Hider, Med. Chem. 47 (2004) 6349–6362.
[44] G.E. Tumambac, C.M. Rosencrance, C. Wolf, Tetrahedron 60 (2004) 11293–11297.
[45] S.J. Ou, Z.H. Lin, C.Y. Duan, H.T. Zhang, Z.P. Bai, Chem. Commun. (2006) 4392–4394.
[46] J.L. Bricks, A. Kovalchuk, C. Trieflinger, M. Nofz, M. Büschel, A.I. Tolmachev, J. Daub, K. Rurack, J. Am. Chen. Soc. 127 (2005) 13522–13529.
[47] K. Kurita, Prog. Polym. Sci. 26 (2001) 1921–1971.
[48] M.N.V. Ravi Kumar, React. Funct. Polym. 46 (2000) 1–27.
[49] C.-M. Lee, D. Jang, J. Kim, S.-J. Cheong, E.-M. Kim, M.-H. Jeong, S.-H. Kim, D.W. Kim, S.T. Lim, M.-H. Sohn, Y.Y. Jeong, H.-J. Jeong, Bioconjugate Chem. 22 (2011) 186–192.